Int. J. Heat Mass Transfer. Vol. 21, pp. 571–580

0017-9310/78/0501-0571 $02.00/0

PREDICTION OF FURNACE HEAT TRANSFER WITH A THREE-DIMENSIONAL MATHEMATICAL MODEL

B. R. PAI,* S. MICHELFELDER† and D. B. SPALDING‡

(*Received* 15 *April* 1977 *and in revised form* 20 *October* 1977)

Abstract—A general procedure for the computation of three-dimensional flows with recirculation, combustion and heat transfer has been recently developed by Patankar and Spalding [2, 6]. The present paper describes an exercise wherein computations based on this procedure are made for the case of the experimental rectangular furnace of the International Flame Research Foundation, Holland. At IFRF, the furnace trials were carried out to provide data with a calorimetric hearth for testing mathematical models of furnaces (M-3A trials). Computations and comparison with experiment are made for the case of a tunnel burner operating on natural gas, firing parallel to the hearth as well as inclined to the hearth, at 25°. It is found that quite realistic predictions of flow and velocity patterns, temperature patterns and hear-flux distributions are obtained with a single set of sub-models which describe turbulent exchange of momentum, mass and heat, and radiative exchange. While discrepancies with measurement exist, the comparison with experiment is encouraging.

NOMENCLATURE

α, gray-gas attenuation coefficient [1/m];
C_1, C_2, C_D, constants in turbulence model;
$C_{P,0T}$, mean specific heat of gas between 0 and T K [J/kg °C];
E_K, constant in law of the wall;
E_H, black-body emissive power of wall [W/m^2];
ε, dissipation rate of turbulence;
ε_H, emissivity of the hearth;
F_x^+/F_x^-, radiative fluxes in the positive and negative x-direction [W/m^2];
k, kinetic energy of turbulence per unit mass [m^2/s^2];
K, constant in the law of the wall:
q_h, heat flux to hearth [w/m^2];
Q_{con}, heat flow due to convection [KW];
Q_{tot}, total heat flow [KW];
σ_h, Prandtl number for laminar diffusion;
σ_{eff}, effective Prandtl/Schmidt numbers for enthalpy, k, ε;
$\eta_{(1-17)}, \eta_{(1-23)}$, heat-transfer efficiency of hearth and total cooling load in furnace respectively;
x, y, z, Cartesian coordinates [m];
μ_{eff}, effective viscosity [kg/m s];
ϕ, any conserved property;
ρ, fluid density [kg/m^3];
Γ_{eff}, effective diffusion coefficient [kg/m s];
S_ϕ, net rate of generation of ϕ [ϕ/s m^3];
t, time [s];
$\mathbf{U}$, velocity vector [m/s];
$\bar{U}_x$, mean velocity in x-direction [m/s];
u, v, w, velocity components in x, y, z direction [m/s].

*National Aeronautical Laboratory, Bangalore, India.
†International Flame Research Foundation, Netherlands.
‡Imperial College of Science and Technology, London, U.K.

1. INTRODUCTION

1.1. *Preamble*

THERE is considerable interest in industrial and academic circles in the prediction of detailed furnace performance starting from the fundamental laws of physics. This is particularly true in applications such as large utility boilers, pre-heat furnaces, etc., where the heat-flux distribution to the charge is required to be calculated, as well as its average value. Simple mathematical models, giving average values of heat-flux in furnace, and hybrid models which predict heat-flux distributions using empirical methods, have been in existence for a long time; recently, however, detailed calculation of the physical processes within the furnace has become feasible, with the aid of high-speed digital computers and developments in numerical procedures. The physical processes occurring inside the furnace include: flow and mixing of the incoming streams and products of combustion; complex chemical reactions; and heat transfer by radiation, convection and conduction. In order to represent the furnace performance, it is therefore necessary to model each of these phenomena, which occur simultaneously within the furnace. Reviews of these procedures may be found for example, in [1, 2].

Most of the work on the validation of prediction procedures has been restricted to two-dimensional furnaces, including axi-symmetric cylindrical furnaces [3–5], partly because no three-dimensional computational program was available until recently. The general conclusion which may be drawn from these efforts is that numerical methods, in combination with fairly simple sub-models for the individual processes, can give realistic predictions over major portions of the furnace of the distribution of quantities such as heat flux, temperature and gas composition. Such discrepancies from experimental data as do arise may be attributed to the deficiencies of sub-models or to departures between the supposed and actual experimental conditions.

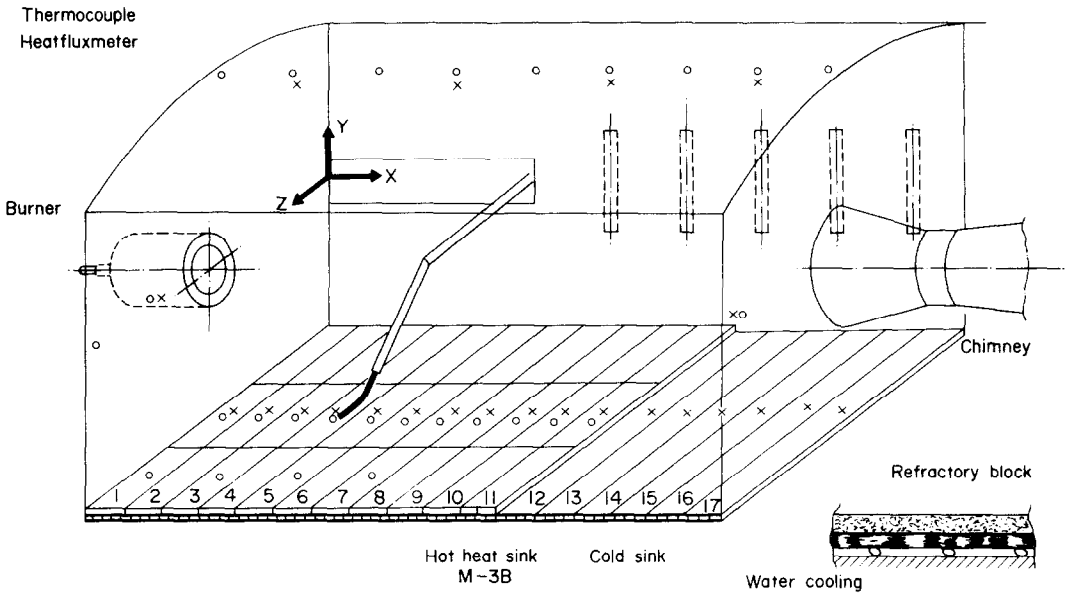

FIG. 1. Experimental furnace for heat-transfer trials (M-3).

In practice, the majority of furnaces are three-dimensional in nature. A general three-dimensional calculation procedure for the solution of the time-averaged Navier–Stokes equations and other conservation equations such as enthalpy, species, etc. has been developed by Patankar and Spalding [2, 6]. This procedure permits prediction of flow, mixing and heat transfer in fairly complex three-dimensional geometries such as, for example, the corner-fired utility boiler. However, no comparison of the results with experimental data was demonstrated in those references. The present paper represents recent efforts by the authors in this direction.

1.2. *Scope of present contribution*

A series of furnace trials was executed recently at IFRF,*[7], one of the objects of which was to provide suitable test cases for validation of mathematical furnace models. Two flame conditions were provided, with a simple burner geometry. The burners used were of the high-velocity "tunnel" type, for which combustion is essentially complete at the exit of the burner. In one case, the burner axis was parallel to the hearth of the furnace; and, in the second case, it was inclined downwards.

The present paper describes computations by a computer program based on [6], for the above-mentioned furnace situations; the results are compared with the results of the M-3A furnace trials at IFRF.

2. EXPERIMENTAL PROGRAMME

The M-3A trials were conducted in the Ijmuiden furnace No. 1, to investigate the influence of operational variables such as fuel type, load, burner type, excess-air ratio and sink type on the heat transfer to a calorimetric hearth. A schematic diagram of the experimental facility is given in Fig. 1.

The furnace comprised a rectangular refractory chamber, approximately 6.3 m long, and 2 m × 2 m in cross-section. The burner was positioned at one end of the furnace. Measurements were made of mean velocity, temperature, gas composition and radiation within the furnace. The "hearth" comprised 17 transverse water-cooled sections, which were insulated from each other, and painted a matt black. By calorimetric measurements on each hearth section, the axial distribution of heat flux to the hearth could be determined. The fuels used included Groningen natural gas, blast-furnace gas, and heavy fuel oil.

To reduce the complexities for the prediction procedure, two flame conditions were set up, from which the effects of combustion and fuel-air mixing could be eliminated as a first approximation. This was achieved by using a high-velocity natural-gas tunnel burner (shown in Fig. 2), for which the combustion was essentially completed at the burner exit. The combustion products entered the furnace without swirl. The burner orientation was horizontal in one case (designated flame 8), and inclined at an angle of 25° in the second case (designated flame 10). The gas velocities at the exit from the tunnel were of the order of 120 m/s; and the nominal thermal input was 3 MW.

During the course of experiment, the furnace was allowed to reach steady conditions for each flame situation; velocity measurements were carried out with a water-cooled 5-hole hemispherical impact probe; gas-temperature measurements were made by a suction pyrometer, gas-composition measurements by chromatographic techniques, and radiation measurements by an ellipsoidal radiometer. Use of special water-cooled, cranked probe-holders permitted the making of these measurements throughout the entire furnace space. Further details of the furnace trials and tabulated data can be found in [7].

*International Flame Research Foundation, Ijmuiden, Netherlands.

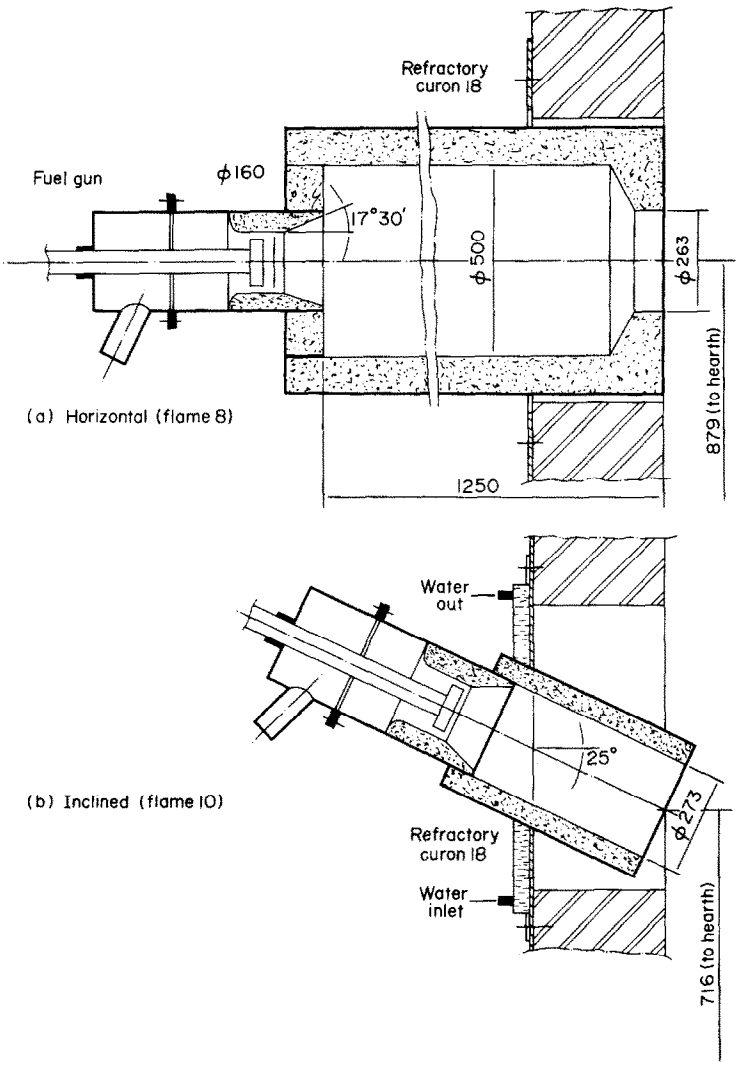

FIG. 2. Design of high-momentum tunnel burners.

3. PREDICTION PROCEDURE

The prediction procedure employed here is based on that described in [6]; it solves the finite-difference equations describing time-averaged, three-dimensional flow, in the presence of recirculation and turbulence, simultaneous with the conservation equations for mass and energy.

3.1. *Governing equations*

The conservation equation of a conserved property ϕ can be written in the form:

$$\frac{\partial \phi}{\partial t} + \mathrm{div}(\rho \mathbf{u} \phi) = \mathrm{div}(\Gamma \, \mathrm{grad}\, \phi) + S_\phi. \qquad (1)$$

The first term indicates the variation with time, and the second represents the convective transport. The terms on the RHS represent the diffusive transport and source term respectively.

In the present problem, the following equations are to be solved:

(i) Conservation of linear momentum in three directions, viz. the x-y-z directions of the Cartesian system. Here ϕ stands in turn for each of the three velocity components u, v, w, and S_ϕ contains the pressure gradient.

(ii) The continuity equation. Here ϕ is identically unity, and S_ϕ equals zero.

(iii) The equations for k and ε, the specific kinetic energy of turbulence and the dissipation rate of turbulence respectively. In these equations, S_ϕ takes special forms which may be found in [8], where the $k \sim \varepsilon$ model is described at some length. These equations are solved in order to obtain the distribution of the effective viscosity. The effective viscosity relates the shear stresses in the fluid to the local gradient of the velocity vector components. For the $k \sim \varepsilon$ model, the definitional relation is:

$$\mu_{\mathrm{eff}} = C_D \rho k^2 / \varepsilon, \qquad (2)$$

where C_D is an empirical constant.

The equation for ε contains two empirical functions C_1, and C_2, which are assigned constant values in the present case. The values assigned to all the empirical constants are given in Table 1.

Table 1. Constants used in calculation

Turbulence							Radiation
σ_h	σ_{eff}	K	E_R	C_1	C_2	C_D	α (1/m)
0.7	0.9	0.4	2	1.43	1.92	0.09	0.2

(iv) The conservation of enthalpy. In this case ϕ stands for h, the enthalpy of the gases. The diffusional transport of enthalpy is again based on the effective exchange coefficient, which is related to the effective viscosity through an effective Prandtl number, σ_h (Table 1). The radiative exchange within the furnace causes significant heat transfer in the furnace and makes its appearance in the enthalpy conservation equation in the source term, S_ϕ.

(v) The radiation transfer, represented by a "6-flux" method. Here ϕ stands for the sums of forward and backward radiation fluxes, as described in [6]. It is further assumed that the gases in the furnace are grey with a constant emission/attenuation coefficient α (Table 1).

3.2. *Boundary conditions*

Boundary conditions must be specified for each independent variable, appropriate to the problem being solved. Since it would be tedious to describe the boundary conditions exhaustively, the salient ones are briefly described below. Further details of boundary condition specification are to be found in [6, 8].

Boundary conditions can be of three general types, viz. specified-value, specified-gradient and mixed types. The specified-value type is applicable for the velocity components (i.e. zero at solid walls and inlet values at the burner nodes), and the k and ε equations. The gradient type is applicable for the pressure correction normal to solid walls; indeed the gradient of the pressure correction normal to solid walls is zero. For the radiation equations, a mixed type of boundary condition is applicable near walls and is derived from the balance equation of the type:

$$F_x^- = \varepsilon_w E_w + (1-\varepsilon_w)F_x^+. \qquad (3)$$

In addition to specification of boundary conditions for variables, special procedures are necessary for calculation of the transport coefficients when the gradients near the wall are large, as in the case, for example, of the velocity components and the enthalpy near a heat sink. The procedure adopted here is to use "wall functions" which relate the transport coefficients to the variable values at near-wall grid points. Such a procedure obviates the need for a large number of grid points in regions of large gradients. It is described in [8].

3.3. *Finite-difference solution procedure*

The differential equations mentioned above are cast into a finite-difference form with reference to a computational grid covering the flow field. The finite-difference equations are obtained by integrating the differential equations over a control volume surrounding each mesh point, assuming a certain profile of the variable in between mesh points. Such a procedure results in a set of algebraic equations, each equation being a "micro-integral" equation around a mesh point. The computational procedure incorporates a number of features which help to achieve a rapid, stable and accurate solution. These features include the use of a "staggered" grid for the storage of velocity components, linearisation of source terms, under-relaxation of variables, etc.

The simultaneous algebraic equations resulting from the finite-difference analysis are solved by a semi-iterative procedure. For each variable, the solution is obtained along one grid line at a time, by use of a tri-diagonal matrix algorithm (TDMA). Repeated scanning of the grid lines in the x, y and z directions causes the converged solution to be gradually approached.

4. SETTING UP OF MATHEMATICAL MODEL

In this section, the steps taken to adapt the general program to the present problem are outlined.

4.1. *Computational grid*

Since there was symmetry about the central vertical plane for both flames, it was sufficient to make the computations for only one longitudinal half of the furnace. A (7 × 12 × 14) non-uniform grid was selected, as shown for the case of flame 10 in Fig. 3. The burner exit was covered by only one mesh point. The program

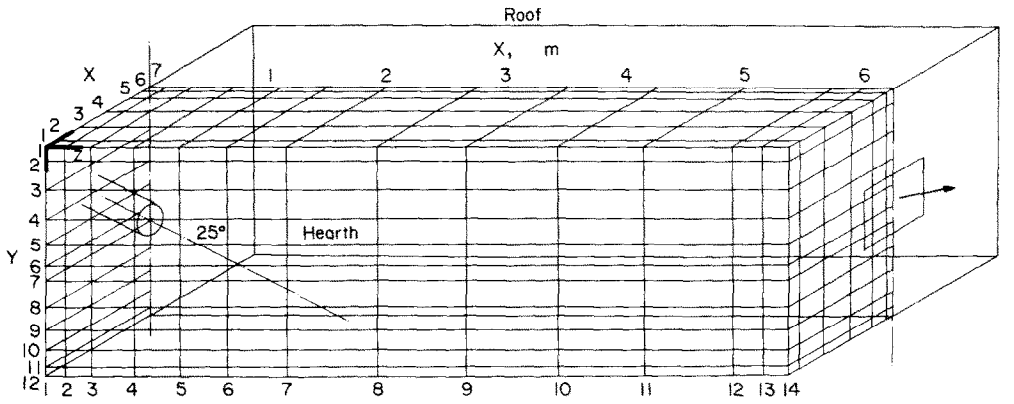

FIG. 3. Computational grid for inclined-burner geometry (M3—flame 10).

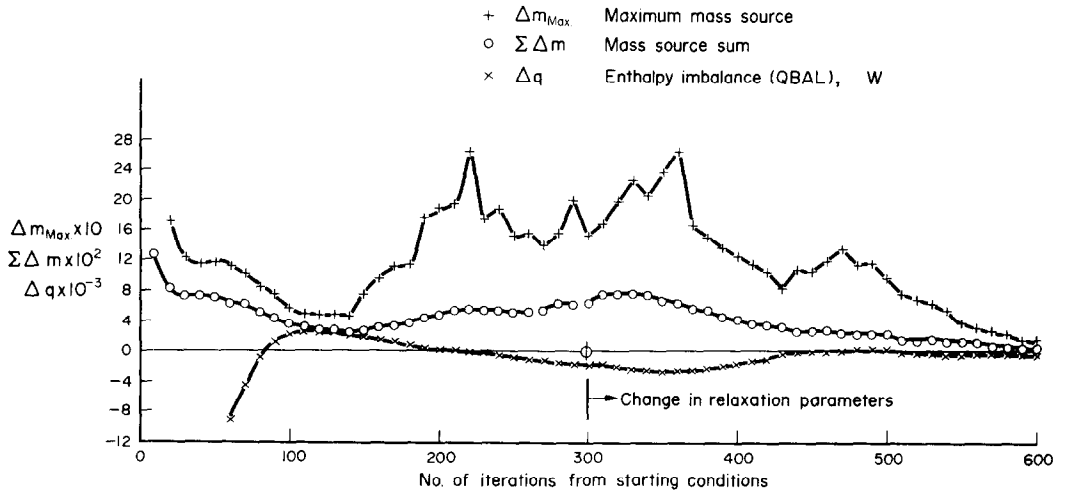

FIG. 4. Variation of convergence parameters.

allows for the difference between the actual flow area of the burner and that of the corresponding control-volume area, and preserves both the mass and momentum fluxes at the specified values. The arched roof of the furnace was approximated by a flat one. In principle, the program can admit boundaries which are not congruent to grid lines, but this refinement was not used.

4.2. *Input flow conditions*

The gases leaving the burner were assumed to be fully burned and at the adiabatic temperature (neglecting dissociation) i.e. 1930°C for 6% excess air: this is higher than the measured one by approximately 200°C. Part of this difference could be ascribed to dissociation, and part to heat loss in the burner.

4.3. *Boundary conditions*

In the experimental furnace, additional cooling loads existed in the form of water-cooled doors for observation slots, distributed on one side of the furnace. The heat removed through these sinks was approximately 11% of the total. A rigorous allowance for these sinks would have increased the complexity of programming, and the running time, unduly, since the assumed symmetry in furnace would be invalidated. Consequently, their presence was allowed for only approximately by increasing the hearth area uniformly by 11%. Further, the refractory furnace walls were assumed to be adiabatic, since the heat loss, estimated from the experiments, was small, namely around 1.5% of the input enthalpy.

4.4. *Physical properties*

The mean specific heat at constant pressure of the furnace gases was assumed to depend linearly on the local temperature. For the combustion products of natural gas, the following relation was presumed.

$$C_{P,0-T} = 1054.1 + 0.1218.T\,(\text{J/kg °C}). \qquad (4)$$

The value for the grey-gas attenuation coefficient was taken as $0.2\ \text{m}^{-1}$ (Table 1). This corresponds to a value based on the mean beam length for the furnace at a mean furnace temperature.

Other physical-property values such as laminar viscosity, Prandtl number, surface emissivities were assigned constant values (viz. 2×10^{-5} kg/ms, 0.7 and 0.88 respectively) appropriate to the problem. The laminar viscosity, of course, was influential only at the wall.

4.5. *Computer system used*

The program was run on a UNIVAC 1108 computer of the UCC System, London. The program as well as intermediate results were stored on disc. This facility permitted calculations to be interrupted and continued later, starting with values from a previous run. Typically, the program took 5.7 s of computer time per iteration for a $(7 \times 12 \times 14)$ grid, when solving the equations mentioned above.

4.6. *Convergence and validity of calculations*

The quantities that were used to monitor the progress of convergence of the calculations were the mass-source sum, maximum mass source and the overall enthalpy imbalance. The first two of these indicate the overall and local deviation from mass conservation and are normalised with the input mass flow. The convergence rate depended on the relaxation factors used. Figure 4 shows the variations of the convergence parameters with the progress of calculation for the case of flame 8. It is seen that some oscillations are present but the calculations finally settle down, particularly after a reduction in the values of the relaxation factors.

Printout of other quantities were also used to check convergence.

Because of the cost of computing, tight convergence limits were not imposed. Table 2, indicates the values of the convergence monitors for which results are presented in the next section. The starting values for these computations were previous computations for which about 800 iterations from uniform starting values were performed. The mass source sum for flame

Table 2. Values of convergence parameters (values are referred to input values of mass flow and enthalpy)

No. of iterations from previous solution	Flame 8 600	Flame 10 300
Mass source sum	6.1×10^{-3}	9.8×10^{-2}
Maximum mass source	1.57×10^{-4}	4.2×10^{-3}
Energy imbalance	1.4×10^{-4}	2.44×10^{-2}

10 is still rather large, but it was found to be decreasing monotonically. The change in values of heat flux was small: less than $\frac{1}{2}\%$ in the last 200 iterations.

5. PRESENTATION AND DISCUSSION OF RESULTS

It is convenient to discuss in turn the predictions of velocities and flow patterns, temperature distributions and heat-transfer quantities. Comparison with experimental data will be made wherever possible.

5.1. *Velocities and flow pattern*

Figure 5a shows the predicted velocity-vector field in the central vertical plane for the case of the horizontal burner (flame 8). The pattern is as expected and contains the central jet region with a recirculation on either side of it. The centre or "eye" of the recirculation lies at a distance of about 2.5 m from the burner on the roof side and about 2 m on the hearth side. Figure 6 shows the predicted and measured values of the axial velocity on the burner axis. Both the measurements and predictions indicate a very short potential region; and the agreement between the two is fair. The discrepancy at the starting station is partly due to the lower density assumed in the calculation, corresponding to use of a temperature which neglects dissociation, and partly due to incomplete combustion and heat losses which reduce the burner exit velocity. It may be noted that the free-jet law, based on the Thring–Newby equivalent jet diameter overpredicts the velocities considerably.

Figure 5b shows the predicted velocity-vector field in the central vertical plane for the inclined-burner case, flame 10. The flow field is as expected and shows a large recirculation region above the jet. The jet downstream of the impingement region spreads laterally into a vortex which then flows through the chimney. This is the reason that no forward velocity is apparent at an axial distance of about 5 m. Near the burner, the jet spread appears somewhat large, particularly under the jet, giving a large "stagnation-point" region. It could be that the grid spacing was not adequate to indicate the recirculation region under the jet accurately. Unfortunately no reliable experimental velocity data are available for this flame to test the predictions.

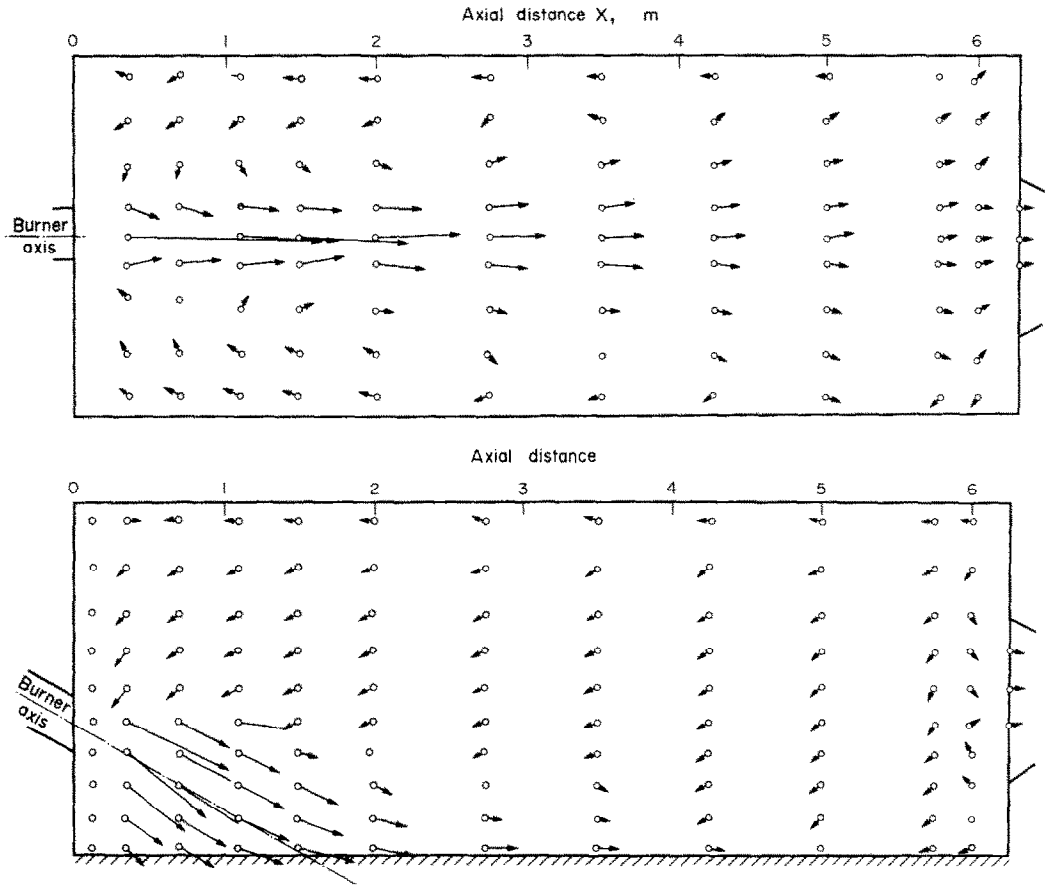

FIG. 5. Predicted velocity field in central vertical plane: (a) flame 8; (b) flame 10.

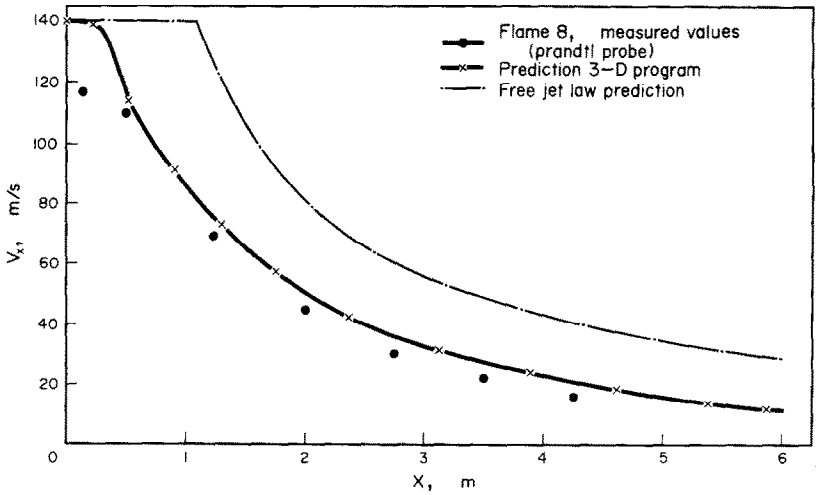

FIG. 6. Predicted and measured axial velocities on jet axis—flame 8 (M-3A trials).

5.2. *Temperature*

Figures 7a and b show the isotherms in the central vertical plane for flame 8, based on measurements and predictions respectively. Figures 8a and b show the corresponding isotherm maps for the inclined-burner case, flame 10. In both cases, the qualitative agreement between the predictions and measurement is good, though some differences of detail exist.

For flame 8, both the measurements and predictions show that the asymmetry caused by the cooled hearth is quite small: the temperatures in the external recirculation regions near the roof and hearth differ by about 100°C. This is mainly because the system is dominated by radiation exchange, which tends to equalise the temperature. The predicted isotherms are somewhat more elongated in the forward jet region than in the experiment; this could be due to the smaller rate of entrainment suggested by the velocity-decay curve (Fig. 6). This causes the temperature of the gases "disentrained" in the downstream half of the furnace to be higher and hence leads to a higher temperature in the external recirculation in the upstream half of the furnace. The implication of this on the heat-flux distribution is discussed below.

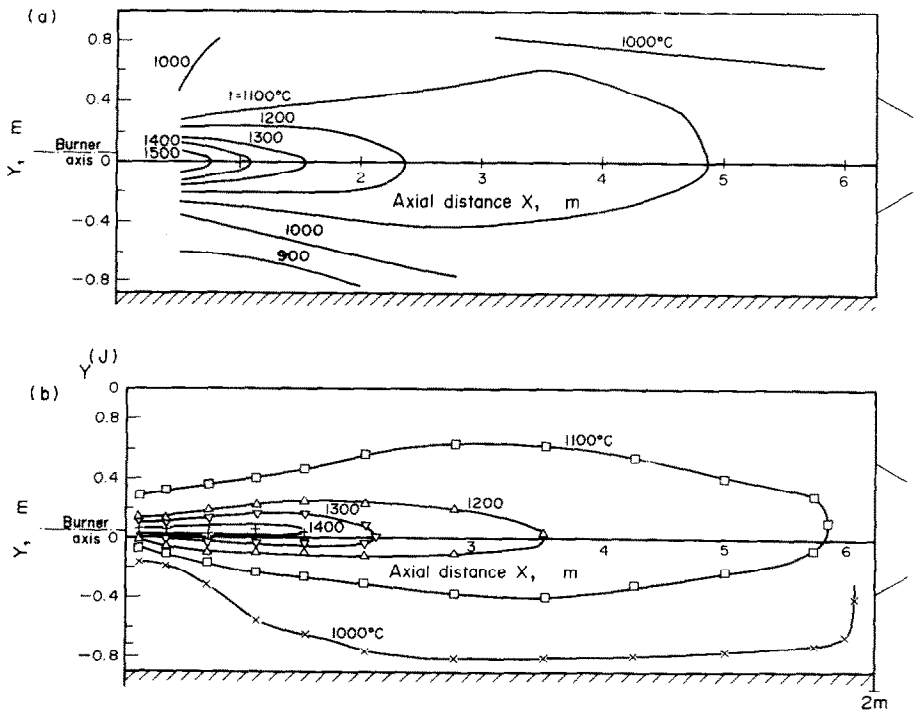

FIG. 7. Isotherms in central vertical plane: (a) based on measurements; (b) predictions from 3-D calculation procedure, M-3A Furnace trials, flame 8.

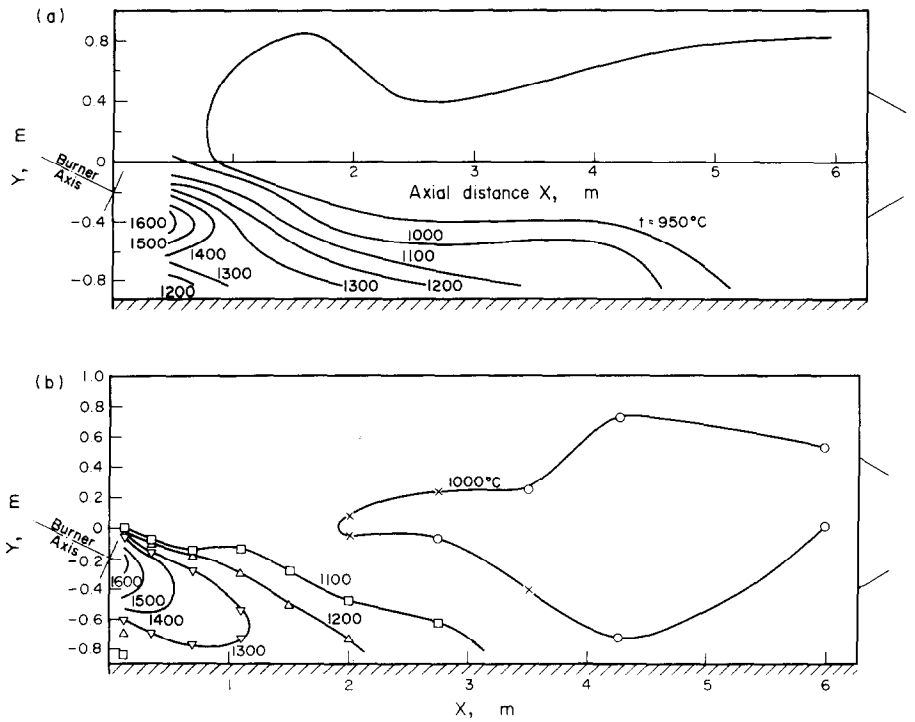

FIG. 8. Isotherms in central vertical plane: (a) based on measurements; (b) predictions from 3-D calculation procedure. M-3A furnace trials, flame 10.

For flame 10, the predicted isotherms near the burner are in fair agreement with the ones based on experiment, but there is an upstream shift in the stagnation region, which was to be expected from the spread in forward-velocity field in Fig. 5b. Both prediction and measurements indicate that the bulk of the furnace space outside the main jet is below 1100°C and above 950°C.

5.3. *Heat transfer*

Table 3 shows the heat-transfer efficiencies for the two flames. Under the measurements column, two efficiencies appear: one based on heat transfer to the 17 hearth segments (η_{1-17}) and one based on the total cooling load, including watercooled doors and burner ring (η_{1-23}). As explained in Section 4.3, these additional cooling loads have been indirectly allowed for in the calculation by increasing the hearth area. This procedure may not be the best one; however, the predicted levels of efficiencies are in good agreement with the measurements. More importantly, the increase in efficiency due to the inclined-burner arrangement is predicted. The predicted increase is somewhat smaller than that indicated by experiment.

Also shown in Table 3 are the ratios of heat transfer by convection to the total heat transferred to the sink. Again the predicted increase in convection is not as much as that indicated by the experiments. No firm conclusion can be arrived at as to the reason. The axial heat-flux distributions for the two flames 8 and 10 are shown in Figs. 9 and 10 respectively. While the heat-flux distribution is relatively flat for flame 8, the pattern is rather peaky for flame 10 due to flame impingement. The level of heat transfer is quite well predicted in the case of flame 8. The rates are slightly over-predicted in the upstream region, as a result of the higher temperatures in the outer recirculation (Fig. 7). In the case of flame 10, while the primary effect of tilting the burner is predicted, the peak value of heat-flux is lower and occurs further upstream than in the experiment. The location of the peak is consistent with the broadening of the stagnation region indicated in the velocity diagram Fig. 5b.

Table 3. Furnace efficiencies

	Based on measurements			Prediction	
	η_{1-17}	η_{1-23}	Q_{con}/Q_{tot}	η	Q_{con}/Q_{tot}
	%	%	%	%	%
Flame 8	45.8	51.8	17	48.5	21.4
Flame 10	52.1	58.4	40	52.5	28.4

6. CONCLUDING REMARKS

The foregoing section has demonstrated that the prediction procedure can make realistic predictions in a practical three-dimensional furnace arrangement, involving turbulent flow with recirculation and heat transfer due to radiation, convection and diffusion. It is true that discrepancies exist between the predictions and measurements, particularly in the case of the inclined burner situation. Further research into the particular sub-models involved in the calculation of

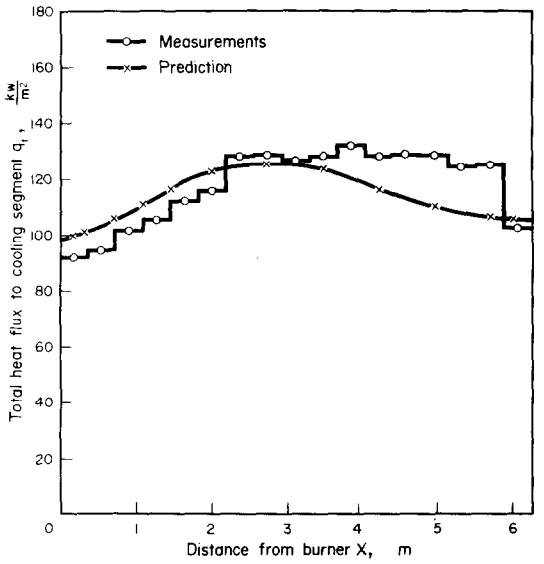

FIG. 9. Predicted and measured heat-flux distribution: M3—flame 8.

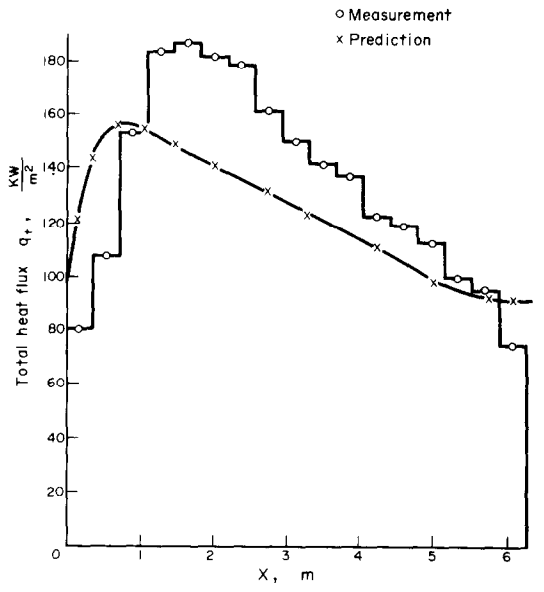

FIG. 10. Predicted and measured heat-flux distribution: M3—flame 10.

convection in inclined impinging jets, and into radiative exchange and property models, will no doubt lead to better agreement with experimental data. However, the capability of the present simple set of sub-models to predict complex changes in a 3-D furnace is encouraging. Further work can be taken up with some confidence, in practical applications where the confinement geometry is more complex, for example, the corner-fired boiler. It would be advisable to introduce complexities such as geometry and reaction kinetics one by one.

Of all the possible causes of discrepancies between predictions and measurements, by far the most probable is the coarseness of the grid, especially in the vicinity of the burner.

Acknowledgement—The authors would like to thank Mr. Serag Eldin for his assistance in setting up the program and to Mr. P. Dale and Mr. B. Faber for assistance with the computer system. The computer program was lent by Concentration, Heat and Momentum Ltd.

REFERENCES

1. S. Michelfelder, W. Richter, B. R. Pai and H. Bartelds, Übersicht über Berechnungsmethoden zur Ermittlung des Wärmeübergangs in Brennkammern, VDI Bericht No. 246 (1975).
2. S. V. Patankar and D. B. Spalding, Mathematical models of fluid flow and heat transfer in furnaces, a review, in *Fourth Symposium on Flames and Industry*, Paper No. 2. Institute of Fuel (1972).
3. T. M. Lowes, H. Bartelds, M. P. Heap, S. Michelfelder and B. R. Pai, Prediction of furnace heat transfer, *15th International Symposium of Combustion Institute at Tokyo* (1974).
4. W. Richter, The predictions of turbulent flows with recirculation and application to a mathematical model of pulverised fuel flames, I.F.R.F. doc. No. F24/ga/5 (1972).
5. P. Hutchinson, E. E. Khalil, J. H. Whitelaw and G. Wigley, The calculation of furnace flow properties and their experimental verification, *J. Heat Transfer* **98C**, 276 (1976).
6. S. V. Patankar and D. B. Spalding, Simultaneous predictions of flow pattern and radiation for three-dimensional flames, in *Heat Transfer in Flames*, pp. 73–94. Scripta Press (1975).
7. B. R. Pai, H. Bartelds and S. Michelfelder, Report on the M-3 Trials, Part A. Cold heat sink. An experimental investigation on the influence of operational and design variables on heat transfer to the furnace hearth, I.F.R.F. Doc. No. F36/a/6 (1975).
8. B. E. Launder and D. B. Spalding, The numerical computation of turbulent flows, *Comp. Meth. Appl. Mech. Engng* **3**, 269–289 (1974).

CALCUL DU TRANSFERT THERMIQUE DANS UN FOUR AVEC UN MODELE MATHEMATIQUE TRIDIMENSIONNEL

Résumé—Une procédure générale de calcul des écoulements tridimensionnels avec recirculation, combustion et transfert thermique a été récemment développée par Patankar et Spalding [2,6]. Cet article décrit l'application de cette procédure à un four rectangulaire, expérimental de la Frif (Hollande). Les essais du four ont été conduits pour obtenir des résultats thermiques qui sont comparés aux prévisions du modèle (M-3A).

La comparaison entre le calcul et les mesures sont faites dans le cas d'un brûleur tunnel à gaz naturel, disposé parallèlement à l'axe du foyer et aussi incliné à 25 degrés. On trouve que les prévisions correctes de la configuration et des vitesses de l'écoulement, du champ des températures et de la distribution du flux thermique, sont obtenues avec un simple système de sous-modeèles qui décrivent les échanges turbulents de quantité de mouvement, de chaleur et de masse, en incluant le rayonnement thermique. Il

Il existe des écarts avec les résultats des mesures mais la comparaison est encourageante

VORHERSAGE DER WÄRMEÜBERTRAGUNG IN EINEM OFEN MIT EINEM DREIDIMENSIONALEN MATHEMATISCHEN MODELL

Zusammenfassung—Ein allgemeines Verfahren zur Berechnung von dreidimensionalen Strömungen mit Rezirkulation, Verbrennung und Wärmeübertragung wurde vor kurzem von Patankar und Spalding [2, 6] entwickelt. Der vorliegende Aufsatz beschreibt eine Anwendung, wobei basierend auf diesem Verfahren Berechnungen für den Fall des rechteckigen Versuchsofens der International Flame Research Foundation in Holland durchgeführt werden. Beim IFRF waren Versuche am Ofen durchgeführt worden, um mit einer kalorimetrischen Feuerstelle Daten zum Testen von mathematischen Modellen für Öfen zu beschaffen (M-3A Versuche). Berechnungen und Vergleich mit dem Versuch werden für den Fall eines mit Erdgas betriebenen Tunnelbrenners durchgeführt, der sowohl parallel als auch unter 25 Grad zur Feuerstelle geneigt feuert. Man fand, daß ganz realistische Vorhersagen des Strömungs- und Geschwindigkeitsbildes, des Temperaturfeldes und der Wärmestromverteilung mit einem einzigen Satz von Teilmodellen erhalten werden, welche den turbulenten Impuls-, Stoff- und Wärmeaustausch und den Austausch durch Strahlung beschreiben. Obwohl Abweichungen von den Messungen bestehen, ist der Vergleich mit dem Versuch ermutigend.

РАСЧЕТ ПЕРЕНОСА ТЕПЛА В ПЕЧАХ С ПОМОЩЬЮ ТРЕХМЕРНОЙ МАТЕМАТИЧЕСКОЙ МОДЕЛИ

Аннотация — Патанкаром и Сполдингом [2, 6] разработана общая методика расчета трехмерных течений при наличии в них процессов рециркуляции, горения и теплопереноса. В настоящей статье дан пример использования этой методики для расчета экспериментальной прямоугольной печи. Для проверки математических моделей используются экспериментальные данные, полученные с помощью подового калориметра. Расчеты и сравнение с данными опытов проведены для туннельной горелки, где природный газ горит параллельно оси топки, а также под углом 25° к ней. Использование единой системы вспомогательных моделей для турбулентного переноса количества движения, массы и тепла, а также лучистой энергии позволяет получить весьма реалистический прогноз картины течения и полей скорости, температуры и тепловых потоков.